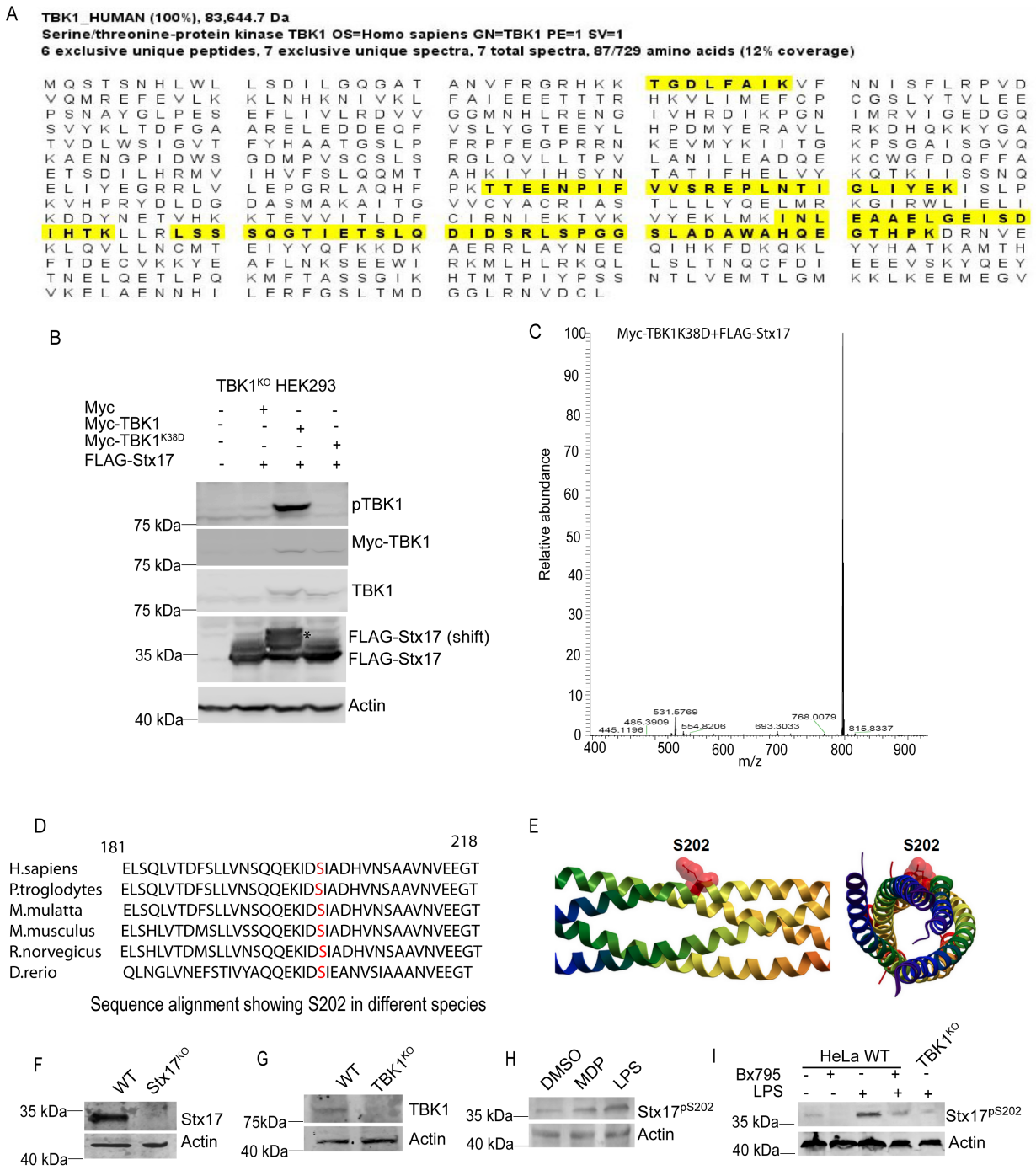

Figure S1, related to Figure 1. TBK1 phosphorylates Stx17. (A) A screenshot captured from the scaffold software indicating number of TBK1 peptides interacting with GFP-Stx17 in proteomics study (related to Figure 1A). **(B)** Western blot from TBK1^{KO} 293T cells expressing Myc, Myc-TBK1^{WT} or Myc-TBK1^{K38D} with FLAG-Stx17. "*" represents phosphorylation-induced shift. **(C)** MS analysis from TBK1^{KO} 293T cells to analyze the effect of Myc-TBK1^{K38D} on FLAG-Stx17 phosphorylation (related to Figure 1C). **(D)** Sequence alignment showing conserved S202 residue in Stx17 from human to

fish. **(E)** Crystal structure from database showing location of S202 in Stx17**. (F)** Western blot confirming Stx17 knock out in $Stx17^{KO}$ HeLa cells**. (G)** Western blot showing TBK1 knock out in $TBK1^{KO}$ HeLa cells**. (H)** Western blot to analyze the effect of MDP or LPS on expression of $Stx17^{pS202}$ in HeLa cells**. (I)** Western blot to analyze the effect of TBK1 agonist LPS and inhibitor BX795 on expression of $Stx17^{pS202}$ in $HeLa^{WT}$ or $TBK1^{KO}$ cells**.**

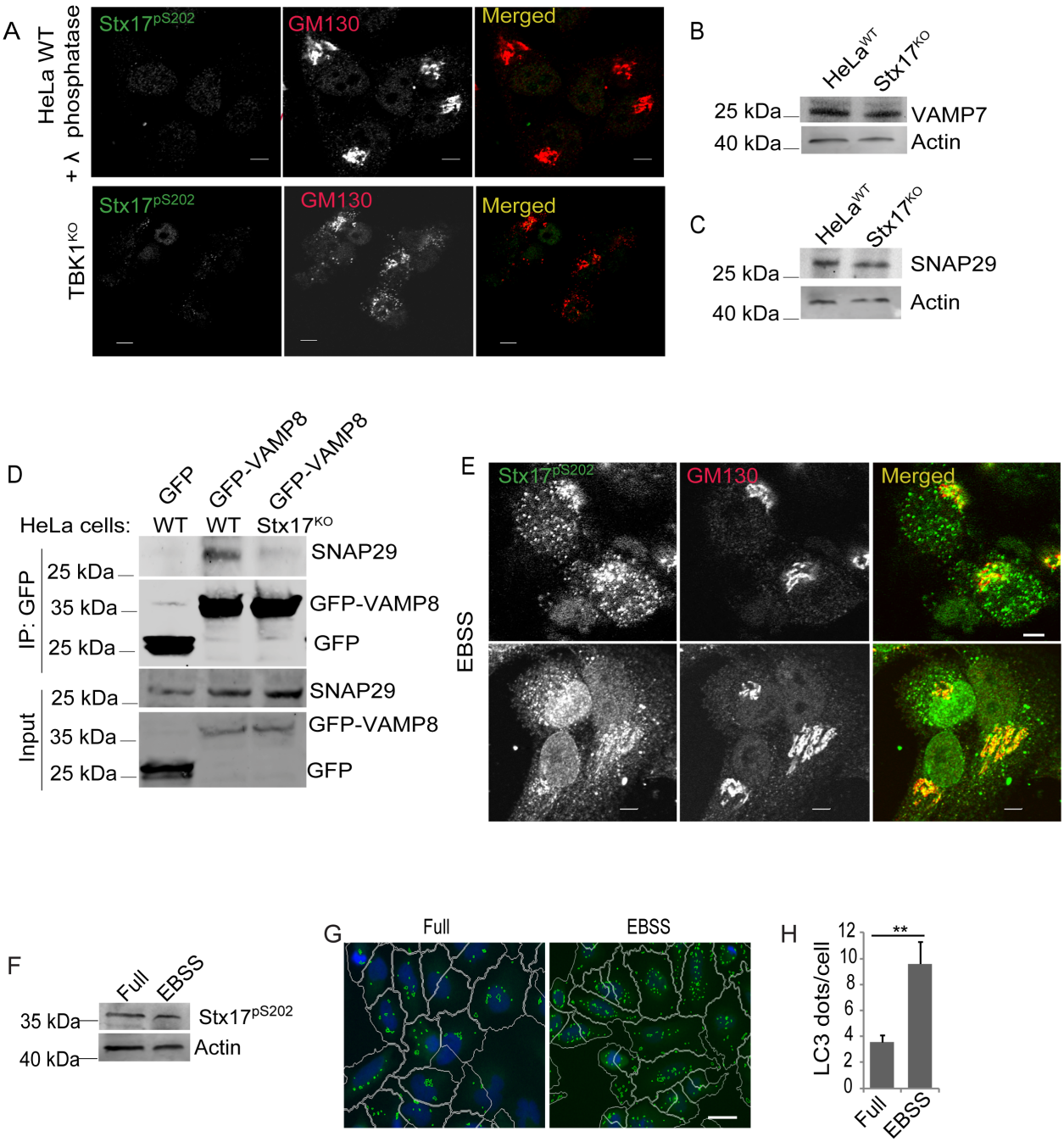

Figure S2, related to Figure 2. Stx17^{pS202} is localized in Golgi. (A) Wild type HeLa cells were treated with ƛ phosphatase (upper row), while TBK1^{KO} HeLa cells (lower row) were left untreated and and stained with Stx17^{pS202} and GM130. Colocalization between Stx17^{pS202} and GM130 was analyzed by confocal microscopy. Scale bar 5 μm. **(B, C)** Western blot to analyze the effect of Stx17^{KO} on stability of VAMP7 or SNAP29. **(D)** Co-IP analysis of interaction between GFP-VAMP8 and SNAP29 in HeLa WT or Stx17 KO cells. **(E)** Confocal microscopy to analyze the distribution of Stx17^{pS202} from Golgi to peripheral dots in response to autophagy induction by EBSS. GM130 is used to stain Golgi. Scale bar 5 μm. **(F-H)** Western blot showing effect of starvation (2h EBSS)

induced autophagy (as shown by induction of LC3 dots in C,D) on levels of Stx17^{pS202}. White masks, algorithm-defined cell boundaries (primary objects); green masks, computer-identified LC3 dots. **, $p < 0.01$, (n=3) t-test.

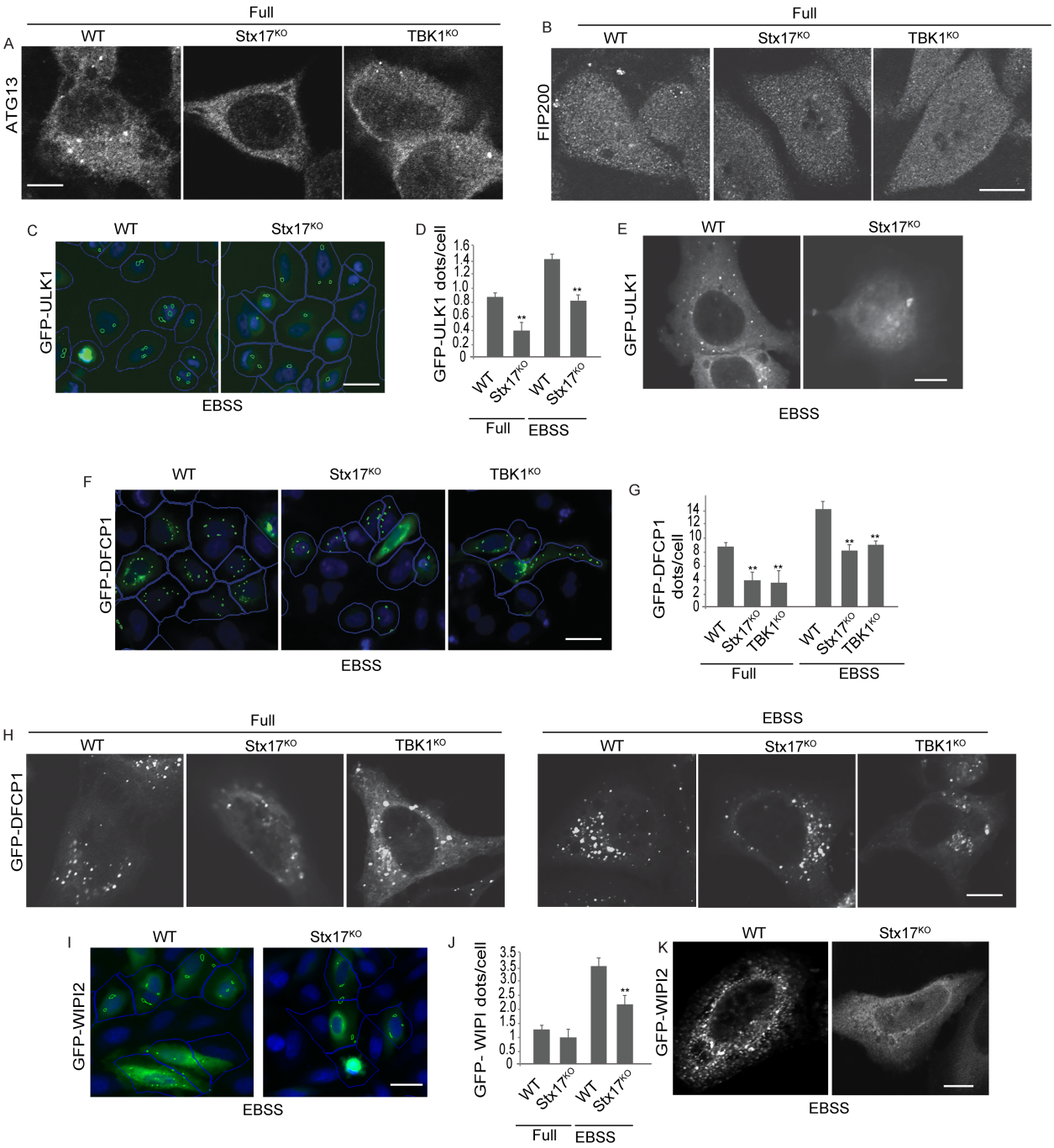

Figure S3, related to Figure 3. Stx17 and TBK1 are required for formation of pre-autophagosomal structures. (A, B) Confocal microscopy analysis of effects of Stx17^{KO} and TBK1^{KO} on formation of ATG13 and FIP200 dots. Scale bar 5 μm. **(C, D)** HC analysis of effect of Stx17^{KO} on formation of ULK1-GFP dots in full media or cells induced for autophagy by incubating in EBSS for 1h. **, $p < 0.01$, (n=3) ANOVA. Blue masks, algorithm-defined ULK-GFP positive cells (primary objects); green masks, computer-identified ULK1-GFP dots. **(E)** Confocal microscopy to analyze the effect of Stx17^{KO} on formation of ULK1-GFP dots. Scale bar 5 μm. **(F,G)** High content microscopy and quantifications showing effect of Stx17 and TBK1 knock outs on

formation of GFP-DFCP1 dots in cells incubated in full media or induced for autophagy by incubating in EBSS for 1h. **, $p < 0.01$, (n=3) ANOVA. Blue masks, algorithm-defined GFP-DFCP1 postive cells (primary objects); green masks, computer-identified GFP-DFCP1 dots. **(H)** Confocal microscopy to analyze the effect of Stx17 and TBK1 knock outs on formation of GFP-DFCP1 dots in cells incubated with full media or induced for autophagy by incubating with EBSS for 1h. **(I, J)** High content analysis showing effect of $Stx17^{KO}$ on formation of GFP-WIPI2 dots in full media or cells induced for autophagy by incubating in EBSS for 1h. Blue masks, algorithm-defined GFP-WIPI2 positive cells (primary objects); green masks, computer-identified GFP-WIPI2 dots. **, $p < 0.01$, (n=3) ANOVA. **(K)** Confocal microscopy to analyze the effect of Stx17 and TBK1 knock outs on formation of GFP-WIPI2 dots.

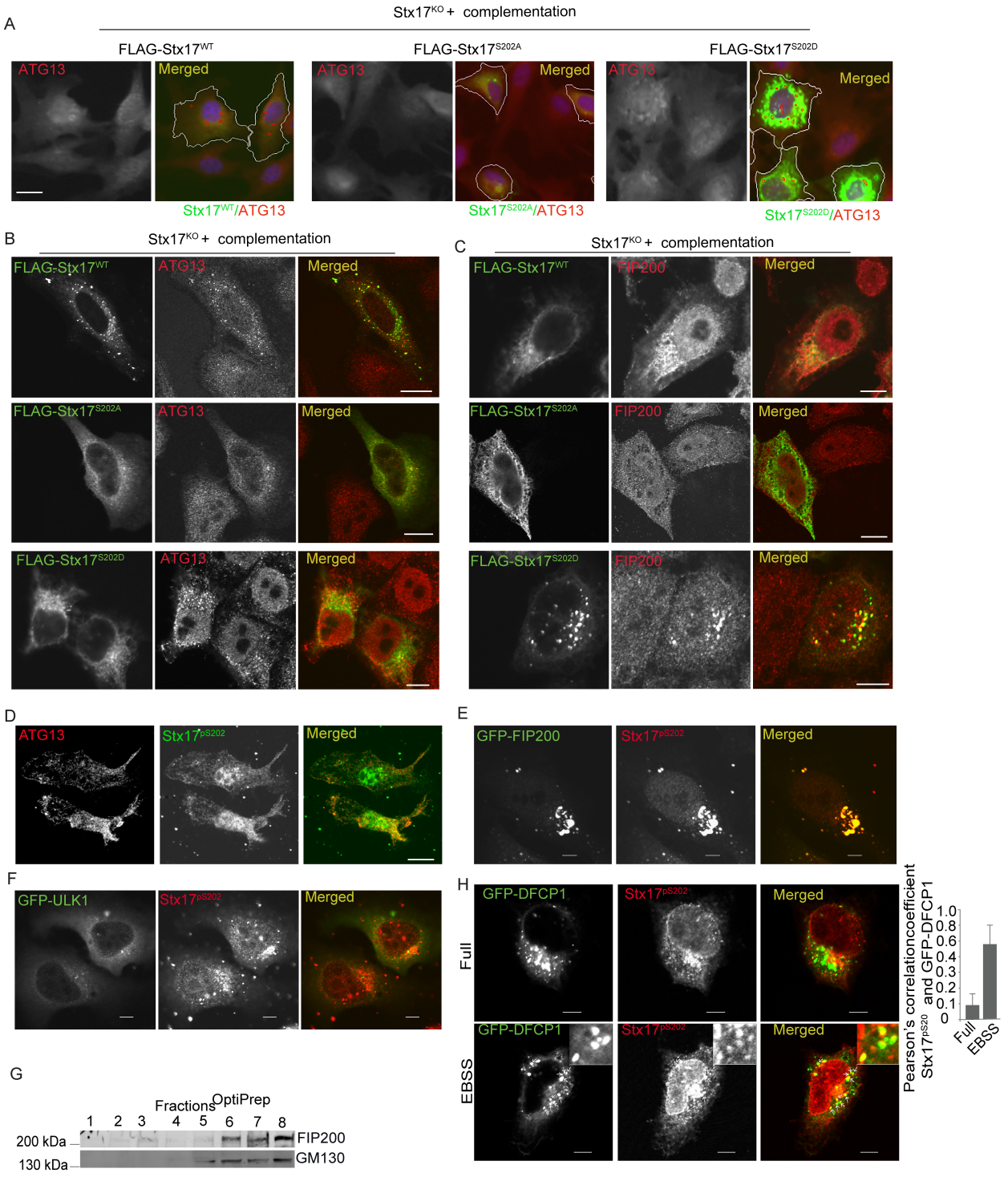

Figure S4, related to Figure 4 and Figure 5. Stx17^{pS202} colocalizes with mPAS. (A) HC images illustrating the effect of complementation Stx17^{KO} cells with FLAG Stx17^{WT}, Stx17^{S202A} and Stx17^{S202D}. Masks: white; FLAG positive cells selected by the machine, red; ATG13 dots in FLAG transfected cells (merged images). Black and white images show unmasked epifluorescence images. White masks, algorithm-defined FLAG positive cells (primary objects); red masks, computer-identified ATG13 dots in FLAG

positive cells. **(B, C)** Confocal microscopy to analyze the effect of complementation of Stx17KO cells with FLAG Stx17^{WT}, Stx17^{S202A} and Stx17^{S202D} on formation of ATG13 (B) or FIP200 (C) dots. Scale bar 5 µm. **(D)** Confocal microscopy analysis of colocalization between ATG13 and Stx17^{pS202} in mouse BMMs. Scale bar 5 µm. **(E)** Confocal microscopy to analyze the colocalization between GFP-ULK1 in and Stx17^{pS202} in HeLa cells grown in full media. Scale bar 5 µm. **(F)** 293T cells were subjected to differential centrifugation and 25 k samples were layered on Optiprep gradients as described in materials and methods. Optiprep fractions were subjected to immunoblotting to analyze co-fractionation of FIP200 with Golgi marker GM130. **(G)** Confocal microscopy analysis of colocalization between Stx17^{pS202} and ULK-GFP in HeLa cell grown in full media. Scale bar 5 µm. **(H)** Confocal microscopy analysis of colocalization between GFP-DFCP1 and Stx17^{pS202} in HeLa cells. Cells were left in full media (upper row) or incubated with EBSS for 1h (lower row). Arrows indicate Stx17^{pS202} and GFP-DFCP1 dots overlapping with each other. Scale bar 5 µm. **(I)** Pearson's correlation coefficient (>20 cells) of colocalization between GFP-DFCP1 and Stx17^{pS202}**.**

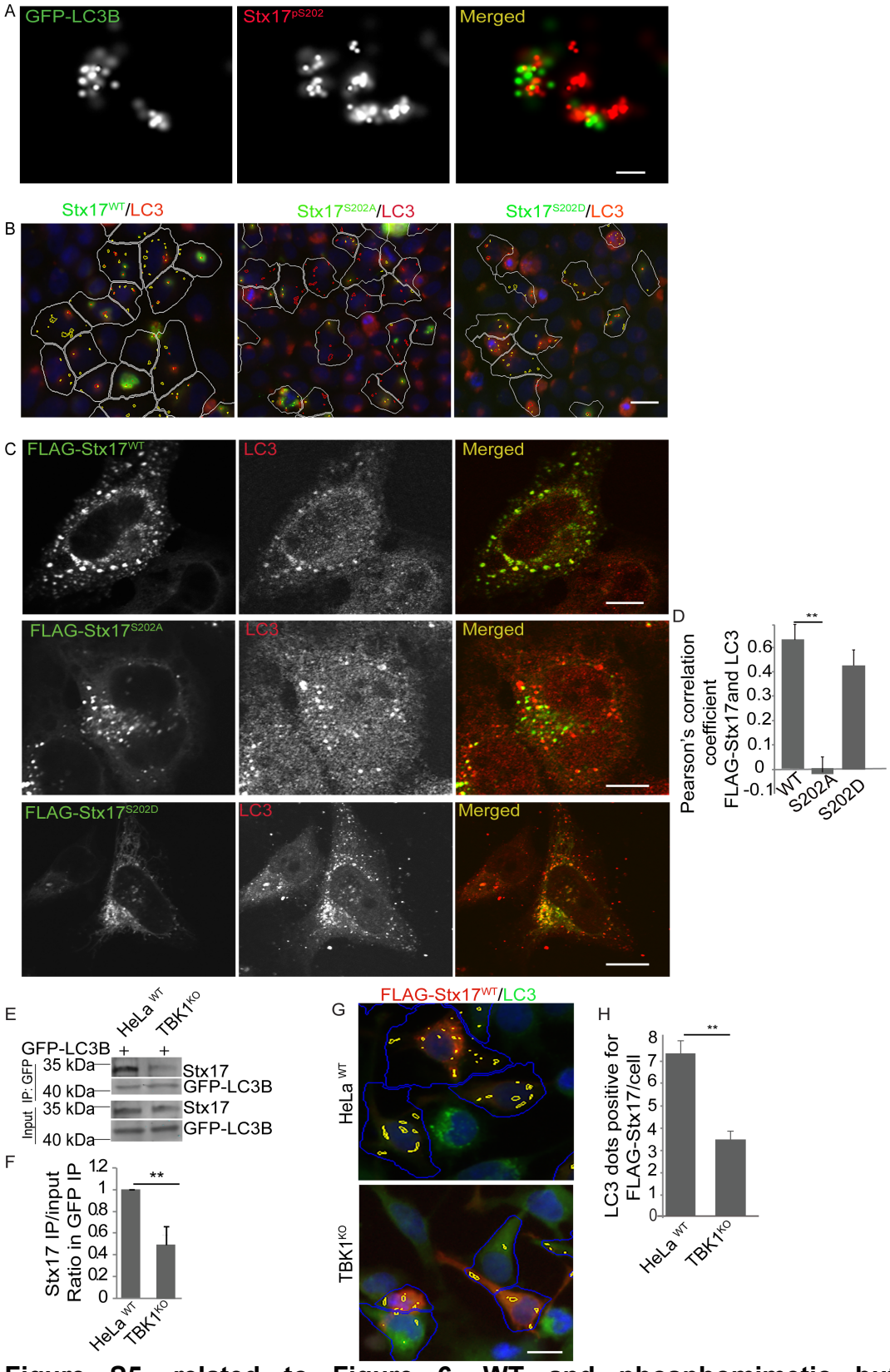

Figure S5, related to Figure 6. WT and phosphomimetic but not non-phosphorylatable Stx17 colocalizes with LC3. (A) Super-resolution microscopy to

analyze the colocalization between GFP-LC3B and Stx17^{pS202} in HeLa cells incubated with EBSS for 2h. Scale bar 500nm. **(B)** HC microscopy to analyze colocalization between FLAG-tagged Stx17^{WT}, Stx17^{S202A} or Stx17^{S202D} mutants with LC3 in cell induced for autophagy with starvation. Scale bar 10 μm. White masks, algorithm-defined FLAG-Stx17 postive cells (primary objects); yellow masks, computer-identified overlap between FLAg-Stx17 and LC3; red, LC3^{+} FLAG^{-} dots. **(C)** Confocal Microscopy to analyze colocalization between FLAG-tagged Stx17^{WT}, Stx17^{S202A} or Stx17^{S202D} mutants with LC3 in cell induced for autophagy with starvation. Scale bar 5 μm. **(D)** Graph showing Pearson's correlation coefficient of colocalization between FLAG-tagged Stx17 variants and LC3. **(E, F)** Co-IP analysis and quantifications of interactions between Stx17 and GFP-LC3B in HeLa^{WT} or TBK1^{KO} cells. $p<0.05$; **, $p < 0.01$, (n=3) t-test. **(G,H)** HC analysis and quantifications of colocalization between FLAG-Stx17 and LC3 in HeLa^{WT} or TBK1^{KO} cells induced for autophagy by incubating with EBSS for 1h. Blue masks, algorithm-defined FLAG-Stx17 postive cells (primary objects); yellow masks, computer-identified overlap between FLAg-Stx17 and LC3. $p<0.05$; **, $p < 0.01$, (n=3) t-test.

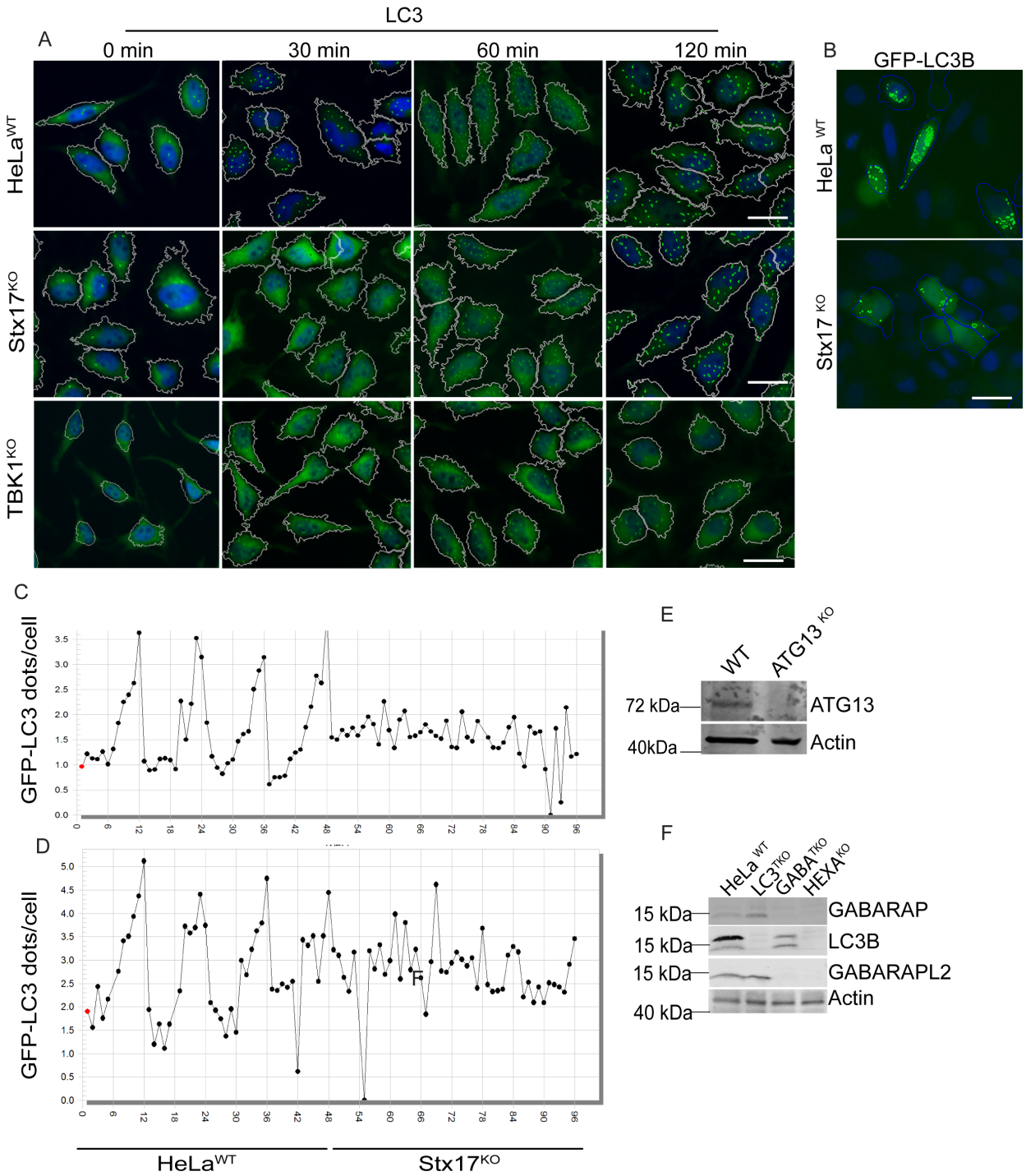

Figure S6, related to Figure 7. Stx17 regulates autophagy initiation (A) HC microscopy to analyze the effect of Stx17 and TBK1 knock out on LC3 puncta formation at indicated time points of autophagy induction by starvation. White masks, algorithm-defined cell boundaries (primary objects); green masks, computer-identified LC3 dots. **(B)** High content images showing effect of Stx17 knock out on GFP-LC3 puncta formation after 1h autophagy induction with EBSS. White masks, algorithm-defined GFP-LC3 positive cells (primary objects); green masks, computer-identified GFP-LC3B dots. **(C, D)** Screenshots of layout of the plates used in Figures 7J and S7B, showing

effect of Stx17 knock outs (right half of the plates) on formation of GFP-LC3B puncta. **(E)** Western blot showing ATG13 knock out in HeLa cells. **(F)** Western blot confirming LC3B, GABRAP and GABARAPL2 knock outs in mATG8s knock out cells.